Gas Separation

DOI: 10.1002/anie.201209077

Stabilization of Low-Temperature Degradation in Mixed Ionic and Electronic Conducting Perovskite Oxygen Permeation Membranes**

Yan Liu, Xuefeng Zhu, Mingrun Li, Huanyin Liu, You Cong, and Weishen Yang**

Mixed ionic and electronic conducting (MIEC) oxides are multifunctional materials used as catalysts,[1] superconductors,[2] fuel-cell and battery electrodes,[3] as well as membranes for gas separation.[4] Among the applications, MIEC membranes with fast transport of oxygen ions at elevated temperature have received increasing attention because the membranes can potentially be used for highly pure oxygen production with low costs; they are highly efficient as membrane reactors for the selective oxidation of C_1 and C_2 molecules,[4g,h] water splitting for hydrogen production reactions,[5] and CO_2 capture integrated with oxy-fuel combustion technology.[6] Despite their widespread use, the high-temperature (usually 800–1000 °C) operation of the membrane modules requires special sealants sustaining high-pressure gradients and special stainless steel resisting high temperatures and oxidation, which have become the bottleneck technology of the application of MIEC membrane technology.[4c] Great energy consumption and high investment on high-temperature membrane modules count against the reduction of the costs for oxygen production. The bottleneck technology is easy to be overcome, as well as the energy consumption and the investment can be significantly reduced at low-temperature (LT; 350–650 °C) operation. Furthermore, many catalytic oxidation reactions of C_3–C_6 organic molecules can be performed in the MIEC membrane reactors with high efficiency at LT.[7]

However, most MIEC materials suffer from large and irreversible performance losses during long-term operation at LT that limit their commercial application.[8] This problem is particularly acute for many of the recent higher-performance perovskite-based MIEC materials such as $Ba_{0.5}Sr_{0.5}Co_{0.8}Fe_{0.2}O_{3-\delta}$ (BSCF)[4a,9] and $La_{1-x}Sr_xCo_{1-y}Fe_yO_{3-\delta}$ (LSCF, $0 \le x \le 1$, $0 \le y \le 1$)[10] that have been designed for low-temperature fuel cells, gas separations, and catalytic processes. Up to now, it is still difficult to stabilize oxygen permeation fluxes of MIEC membranes at LT. In general, degradation processes of materials become more severe with increasing temperature. Thus, the fact that MIEC membrane degradation becomes more severe at lower temperatures stands in stark contrast to the conventional wisdom. Two main mechanisms have been proposed to account for the LT degradation in perovskite MIEC membranes. The first is that oxygen vacancy ordering occurs in these materials during sustained operation at LT, which severely decreases their ionic conductivity;[10] the second is that LT operation introduces thermodynamic driving forces that favor kinetic demixing in these materials under oxygen permeation conditions, producing new phases with low ionic conductivity or undesirable changes to the surface elemental composition and morphology.[11] However, these two proposed mechanisms cannot explain why degradation is observed even in many otherwise structure-stable membranes, for example $BaZr_xCo_yFe_{1-x-y}O_{3-\delta}$.[4b,12]

Here, we identify a third important and potentially widespread degradation mechanism related to the operation-induced surface segregation of trace impurities of sulfur that appears to dramatically impact the LT permeation behavior of perovskite-type MIEC membranes. Based on this finding, we propose a simple but remarkably effective method that for the first time enables the stabilization of permeation fluxes of perovskite MIEC membranes at LT. We apply this strategy to a number of recently developed high-performance LT perovskite-type oxygen permeation MIEC membranes including $BaCe_{0.1}Co_{0.4}Fe_{0.5}O_{3-\delta}$ (BCCF),[13a] $BaCo_{0.7}Fe_{0.22}Nb_{0.08}O_{3-\delta}$ (BCFN),[13b] and $BaZr_{0.2}Co_{0.4}Fe_{0.4}O_{3-\delta}$ (BZCF)[4b] and demonstrate stable oxygen permeation fluxes as high as about 0.5 mL cm^{-2} min^{-1} at 600 °C with degradation of less than 5% after 480 h of operation as compared to the typical 80% degradation experienced in nonstabilized MIEC membranes under identical conditions.

BCCF, BZCF, and BCFN are recently developed perovksite-type MIEC membranes that show a particularly promising oxygen permeation performance, with stable behavior as long as the operation temperature is higher than 750 °C;[4b,13] however, for all three membrane materials derived from high-purity precursors, their permeation flux decreases quickly with time at 600 °C (see Figure 1a and Figure S1 in the Supporting Information). After about 480 h of operation at 600 °C, the permeation flux of BCCF decreases by about 80%, while after just 100 h of operation at 600 °C the permeation fluxes of BZCF and BCFN decrease by 38.5% and 55.7%, respectively. The perovskite structure of the three materials is stable under the operation conditions, and no

[*] Y. Liu, Dr. X. F. Zhu, Dr. M. R. Li, H. Y. Liu, Y. Cong, Prof. Dr. W. S. Yang
State Key Laboratory of Catalysis
Dalian Institute of Chemical Physics, Chinese Academy of Sciences
457 Zhongshan Road, Dalian 116023 (China)
E-mail: zhuxf@dicp.ac.cn
yangws@dicp.ac.cn
Y. Liu, H. Y. Liu
University of Chinese Academy of Sciences
Beijing, 100039 (China)

[**] This work is supported by the NSFC (grant number 21271169/21061130534) and the Fund of the State Key Laboratory of Catalysis (grant number R201107). We also thank Prof. Ryan O'Hayre for his suggestion and comments and the Chinese Academy of Sciences Visiting Professorships (grant number 2012T1G0015).

Supporting information for this article is available on the WWW under http://dx.doi.org/10.1002/anie.201209077.

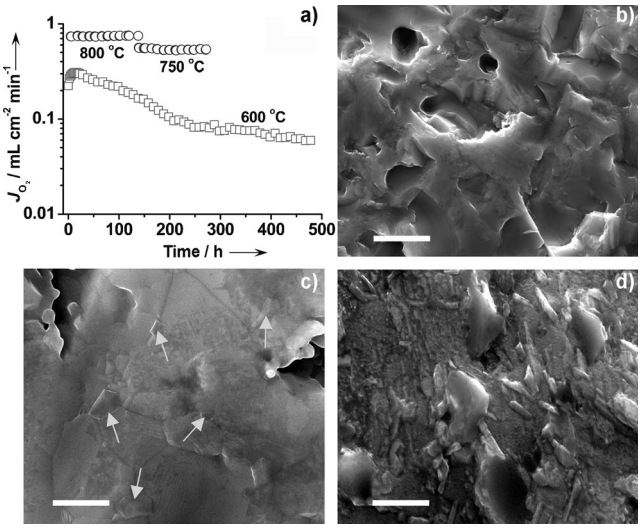

Figure 1. a) Time-dependent oxygen permeation fluxes of BCCF membranes at 800, 750, (thickness: 1.0 mm) and 600 °C (thickness 0.5 mm). b) Surface of the as-prepared BCCF membrane after polishing. c) Feed-side surface and d) permeation-side surface of the spent membrane after 480 h of operation at 600 °C; the arrows show the $BaSO_4$ grains on the feed-side surface; all the protuberant grains on the permeation-side surface are $BaSO_4$. Scale bar: 1 μm.

phase changes are detected even after prolonged aging at high temperature in a pure N_2 atmosphere as determined by in situ X-ray diffraction (XRD; see Figure S2). Therefore, oxygen-vacancy ordering can be ruled out as a source of the flux degradation observed in these materials. The crystalline structures of the three membranes were also investigated by XRD after the long-term permeation tests at 600 °C. All three membranes retained phase purity in the bulk material. However, $BaSO_4$ was detected on all membrane surfaces (see Figure S3) even though all membrane were derived from high purity precursors (containing < 20 ppm sulfur); furthermore, in all cases the intensity of the $BaSO_4$ peaks was significantly higher on the permeate side as compared to the feed side. For BZCF, both $BaSO_4$ and $Zr(SO_4)_2$ impurity phases were detected on the permeate-side surface. However, evidence for decomposition or kinetic de-mixing of the perovskite phase was not observed, nor did we detect the presence of the typical low-conductivity phases (e.g. hexagonal and lamellae phases) that are commonly attributed to LT degradation in sister MIEC materials such as $Ba_{0.5}Sr_{0.5}Co_{0.8}Fe_{0.2}O_{3-\delta}$.[4a,9] Based on these initial findings, additional studies were therefore carried out to further investigate the $BaSO_4$ surface impurities as a potential new explanation for permeation degradation in these systems at LT.

The surface morphologies of the spent BCCF membrane compared with the fresh membrane are shown in Figure 1 b–d. As shown in the figure, after 480 h of operation at 600 °C, there are only slight changes on the morphology of the feed side (see Figure 1 c) with the appearance of sparsely distributed small $BaSO_4$ grains (0.1–1 μm, composition verified by energy dispersive X-ray spectroscopy (EDX), see Figure S4) on the membrane surface. In contrast, the morphology of the permeate side changes remarkably (see Figure 1 d). A large number of protuberant grains all found to be $BaSO_4$ as verified by EDX are distributed all over the membrane surface, and the overall sulfur content on the surface reaches about 2.2 at. %. The enrichment of $BaSO_4$ in the permeate side versus the feed side is also corroborated by the XRD patterns shown in Figure S3a. A similar phenomenon was observed on the surfaces of the BCFN and BZCF membranes as well (see Figure S5). $BaSO_4$ is chemically inert towards oxygen activation and transport; therefore, we think that the enrichment of $BaSO_4$ on the membrane surface can significantly degrade the oxygen exchange rate and block the transport of oxide ions from the bulk to the surface.

The focused ion beam (FIB) technique was used to extract a slice (about 100 nm thick) from the permeate side of the spent BCCF membrane. High-resolution transmission electron microscopy (HRTEM) analysis of the sample enabled detailed investigation of the interfaces between perovskite grains, as well as the interfaces between $BaSO_4$ and perovskite grains, and also the crystalline structure of the surface not covered by $BaSO_4$ (see Figure 2). Selected area electronic diffraction (SAED) analysis and corresponding HRTEM

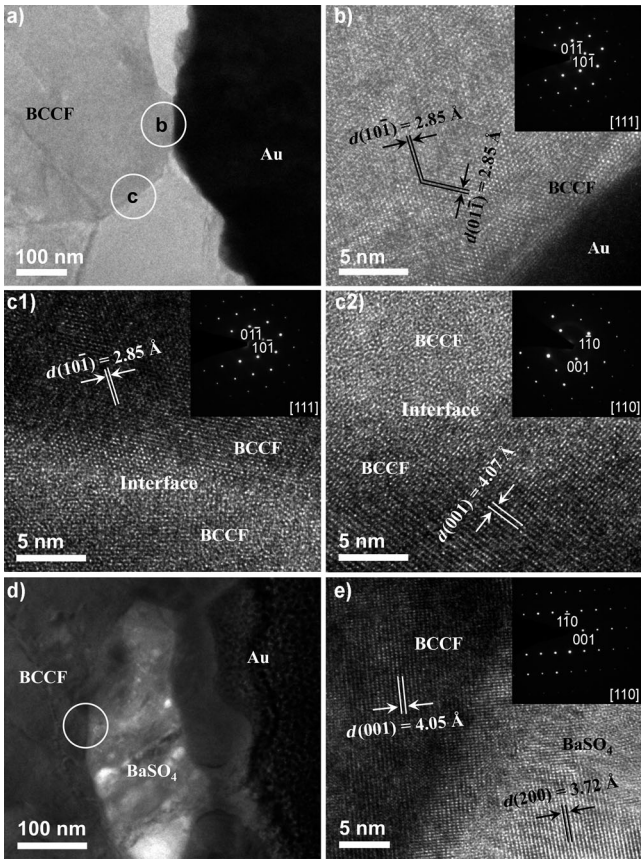

Figure 2. HRTEM analysis of the perovskite membrane after long-term operation at 600 °C. The circles highlighted in the large-scale images (a,d) correspond to the areas shown at higher resolution in (b,c, and e). a,b) "Clean" area of the BCCF surface not covered by $BaSO_4$. c1,c2) High-resolution close-up of a perovskite grain boundaries viewed along the [111] (c1) and [110] (c2) directions. d,e) Grain boundary between the perovskite and $BaSO_4$ viewed along the [110] direction of the perovskite.

images along the [111] direction (Figure 2b provides a representative example) reveal that the surface of the BCCF membrane retains the cubic perovskite structure after long-term operation. The inter-planar spacings measured for the $(10\bar{1})$ and $(01\bar{1})$ planes are similar to those obtained from XRD. The analysis of the interfaces between perovskite grains (a representative example is shown in Figure 2c1,c2) indicates that the grain boundaries are clear and there is no evidence of secondary phases between grains. This is in contrast to the situation in BSCF membranes, where rapid permeation flux degradation at intermediate temperatures has been correlated to the appearance of new phases with low ionic conductivity at the grain boundaries.[9] Interfaces between the perovskite and the $BaSO_4$ surface impurity phase are also clear (see Figure 2e for a representative example), and again there is no evidence for other phases occurring in the grain boundaries.

The starting sulfur impurity content in the BCCF membrane was determined to be less than 20 ppm based on the analysis shown in the Supporting Information, and so it is perhaps at first surprising that this small background impurity content is sufficient to cause such a large and rapid surface exsolution of $BaSO_4$ and a commensurate large and rapid degradation of the permeation flux of the membrane during LT operation. To further verify that sulfur was indeed responsible for this behavior, new perovskite membranes were fabricated that were purposefully enriched with a higher sulfur impurity concentration (marked as BCCF-s, the sulfur content in these membranes was about 135 ppm). These membranes with high sulfur content were subjected to various durability tests, including one membrane that was subjected to LT operation at 650 °C for 100 h, another that was subjected to high-temperature operation at 900 °C for 100 h, and a third that was subjected to high temperature operation at 900 °C for 100 h followed by LT operation at 650 °C for 100 h. The permeation versus time behaviors of the three membranes are shown in Figure 3 along with representative SEM images and EDX analysis. For the membrane subjected to LT operation only, the permeation flux decreases by about 70% (see Figure 3d) and the permeate-side surface of the spent membrane is almost completely covered by a layer of $BaSO_4$ grains after 100 h of operation (see Figure 3a and Figure S6). The sulfur content of the surface reaches 7.5 at.%. Interestingly, when identical membranes were subjected to aging experiments in a single atmosphere of either flowing air or flowing He at 650 °C for 100 h, only a few $BaSO_4$ grains could be found on the membrane surface and the sulfur enrichment on the surface was dramatically lower compared to the case of membranes subjected to permeation testing (see Figure S7). These findings, coupled to the fact that the sulfur content is always dramatically enhanced on the permeate side relative to the feed side under permeation test conditions strongly suggest that the transfer of sulfur from the bulk membrane material to the surface is driven by the chemical potential gradient of oxygen. The probable mechanism of sulfur transport is discussed in detail in the Supporting Information (see Figure S8). This mechanism suggests that sulfur migrates as sulfate species in the same direction as the majority oxygen-ion conduction.

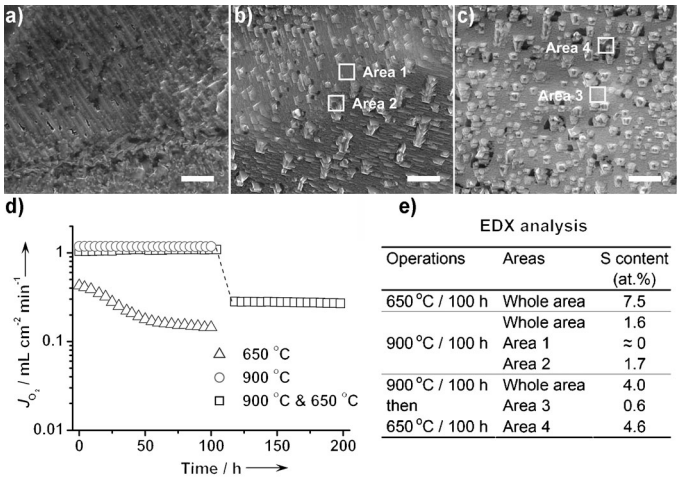

Operations	Areas	S content (at.%)
650 °C / 100 h	Whole area	7.5
900 °C / 100 h	Whole area	1.6
	Area 1	≈ 0
	Area 2	1.7
900 °C / 100 h then 650 °C / 100 h	Whole area	4.0
	Area 3	0.6
	Area 4	4.6

Figure 3. Analysis of the high sulfur-containing BCCF-s membranes operated under different conditions. SEM pictures of the spent membrane surfaces (permeate side) after oxygen permeation testing at a) 650 °C for 100 h; b) 900 °C for 100 h; c) 900 °C for 100 h then 650 °C for 100 h. d) Oxygen permeation flux versus time behavior of the three membranes (1 mm in thickness). e) EDX analysis of the three membranes. Scale bar: 2 μm.

In spite of their high sulfur content and poor LT permeation flux stability, the BCCF-s membranes show an excellent high-temperature permeation stability (see Figure 3d). This is consistent with the observations from other perovskite-type MIEC membrane materials, which typically show good permeation stability above 850 °C.[4,13] After 100 h of operation at 900 °C, the surface of the permeate side of the membrane was analyzed by SEM/EDX and XRD (see Figure 3b and Figure S9). Compared to the membrane operated at 650 °C with an averaged surface sulfur content of 7.5 at.%, the membrane operated at 900 °C had an averaged surface sulfur content of only about 1.6 at.%. This finding is corroborated by XRD analysis, which shows that the $BaSO_4$ diffraction peak intensities decreases significantly for the membrane operated at 900 °C compared to the membrane operated at 650 °C (see Figure S6). For the BCCF-s membrane operated at 900 °C for 100 h followed by operation at 650 °C for an additional 100 h, the permeation flux at 900 °C is very stable as that of the second membrane. Interestingly, however, the permeation flux only decreases slowly during the subsequent 100 h of operation at 650 °C, (see Figure 3d). The concentration of the surface sulfur for the BCCF-s membrane after the combined 900 and 650 °C permeation tests is higher than that of the membrane operated only at 900 °C, but is lower than that of the membrane operated only at 650 °C (see Figure 3c and e).

Thermodynamic calculations reveal that $BaSO_4$ can gradually decompose at elevated temperature (see Figure S10), and the equilibrium constant of the decomposition reaction increases exponentially with temperature. If it is assumed that the bulk sulfur diffusion and surface $BaSO_4$ decomposition kinetics are fast enough to maintain the SO_2 partial pressure in equilibrium with the flowing gas phase, it would take more than 4000 days at 600 °C to remove all sulfur from a 0.5 mm thick BCCF membrane (containing < 20 ppm

S) derived from high purity precursors. In contrast, at 900 °C it would take less than 1 day to accomplish the same thing.

Based on this conceptual exercise, we think that the decomposition of $BaSO_4$ (and hence the ability to remove sulfur from the membrane as SO_2) is thermodynamically and kinetically limited at lower temperatures, thereby explaining why the membranes operated at 650 °C accumulate a higher surface sulfur content. At low operating temperatures, the rate of the enrichment of $BaSO_4$ on the membrane surface is faster than $BaSO_4$ decomposition; as a result $BaSO_4$ grains aggregate on the membrane surface leading to the degradation of the permeation flux. At higher temperatures, even though sulfur segregation from the bulk to the surface should also be accelerated, this is more than offset by significantly faster $BaSO_4$ decomposition, and as a result only a few $BaSO_4$ grains can be found and no degradation of the permeation flux is observed. This mechanism also helps to explain the improved LT flux stability observed for the membrane that was first operated at 900 °C before being operated at 650 °C, as much of the sulfur was likely already removed from this membrane during the first 100 h of operation at 900 °C. It is likely that the mechanism proposed above is not just limited to barium-containing materials. The permeation stability of other membranes containing alkaline-earth and rare-earth elements will also likely be degraded by sulfur impurities since their sulfates are also generally stable at low temperature.

Based on the above analysis, the two-stage flux degradation observed in Figure 1 a (first rapid, then slower) is attributed to rapid aggregation of $BaSO_4$ from the bulk to the surface during the first 200 h of operation followed by slower degradation during continued operation. The degradation rate presumably decreases because of 1) a reduced driving force for the continued surface segregation of sulfur as sulfur is depleted from the bulk and $BaSO_4$ accumulates at the surface, and 2) the gradual decrease of the electronic current. One option to combat the sulfur-induced degradation phenomenon at LT would be to synthesize perovskite membranes using ultrahigh purity sulfur-free reagents. However, recall that even the 20 ppm sulfur impurity level introduced by high-purity reagents used to synthesize the membranes tested in Figure 1, was still sufficient to cause significant degradation. Obtaining still higher-purity reagents, especially at an industrially relevant scale, is not an easy or cost-effective approach. As an alternative, we examined the possibility of deploying a high surface area buffer/catalyst layer with high oxygen activity on both the feed and permeate faces of the membrane to mitigate the effects of the $BaSO_4$ surface contamination.

Porous $Sm_{0.5}Sr_{0.5}CoO_{3-\delta}$ (SSC) was used for this purpose. SSC is a perovskite oxide that shows high oxygen catalytic activity and is commonly used as an oxygen exchange catalyst in MIEC membranes and as a cathode material for low-temperature (about 600 °C) solid oxide fuel cells.[14] A porous SSC composed of particles of 0.5–1 μm in diameter calcined at 950 °C was applied to both sides of a BCCF membrane to create porous surface buffer layers of about 10 μm in thickness. Figure 4 compares the permeation flux stability of the SSC-coated membrane to an uncoated membrane under identical testing conditions at 600 °C. The flux degradation

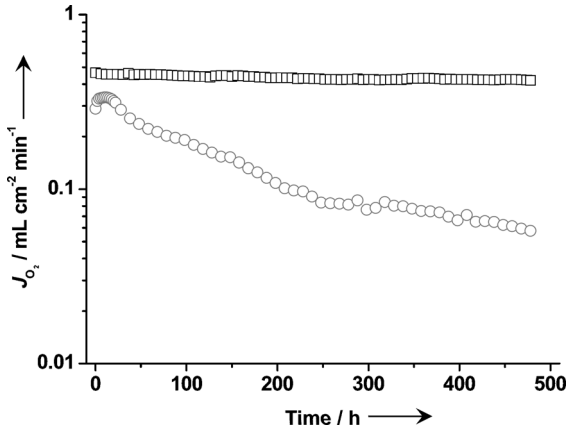

Figure 4. Long-term low-temperature (600 °C) oxygen permeation testing of the uncoated BCCF perovskite membrane (circles; this data is similar to that shown in Figure 1 but obtained for another membrane), and the same BCCF perovskite membrane (squares) with both surfaces coated by SSC porous catalyst layers.

behavior of the uncoated BCCF membrane is similar to what was observed previously for the membrane shown in Figure 1, with an 80 % decrease in flux after 480 h of operation. In contrast, the flux of the SSC-coated membrane decreased by only about 5 % in the first 200 h and then maintained a stable performance. Similarly, a stabilized LT permeation performance was obtained on SSC-coated BCFN and BZCF membranes (see Figure S11). For the SSC-coated BCFN membrane, an 8 % decline in flux was observed in the first 40 h of operation followed by no further decreases in flux over the next 160 h. For the SSC-coated BZCF membrane, a fully stable performance was observed with only small fluctuations of ± 4 % in the flux during 100 h of operation. Our success in achieving flux stabilization in all three perovskite MIEC membrane materials suggests that the SSC-coating stabilization technique may be of widespread use to overcome the LT degradation of permeation flux for many MIEC perovskite membrane material families. To gain further insight into the stabilization mechanism of the SSC-coating, SEM and EDX analyses were conducted on the spent SSC-coated BCCF membrane after 480 h of operation (see Figure 5). This analysis indicates that the $BaSO_4$ grains diffuse to the outer shell of the porous SSC layer and as a consequence, there are no $BaSO_4$ grains remaining on the BCCF membrane surface itself (see Figure 5 d). This finding further verifies that the transport of sulfur is driven by chemical potential gradient of oxygen, and that the SSC coating can effectively act as a "buffer" or a sponge to remove the $BaSO_4$ grains from the membrane surface. Furthermore, thanks to the high surface area and high activity of this porous SSC layer, the enrichment of $BaSO_4$ on the SSC surface has little effect on the oxygen exchange rate as the $BaSO_4$ particles are distributed over a much larger area and cannot completely block the oxygen exchange process. As a result, it appears that the porous SSC buffer layer can be used to maintain a highly stable permeation flux even under low-temperature operation conditions.

In summary, for the first time we report an approach to achieve high and stable oxygen permeation at LT (600 °C) in

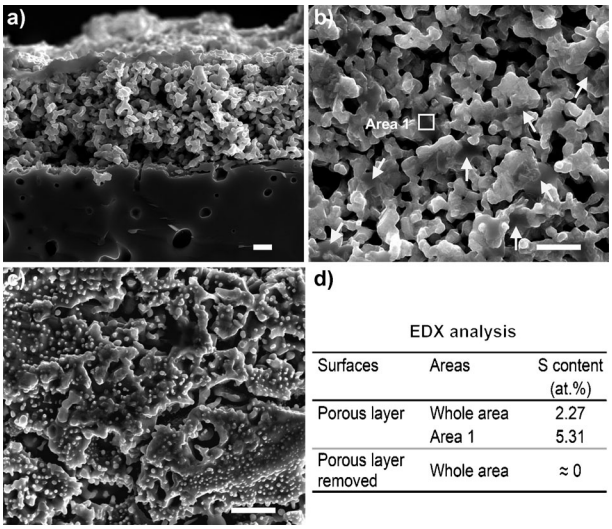

EDX analysis

Surfaces	Areas	S content (at.%)
Porous layer	Whole area	2.27
	Area 1	5.31
Porous layer removed	Whole area	≈ 0

Figure 5. Post treatment and analysis of the SSC-coated perovskite membrane after 480 h of oxygen permeation testing at 600 °C. a) Cross-section view of the porous SSC catalyst layer. b) Top view of the porous SSC catalyst layer. The arrows mark $BaSO_4$ grains. c) Top view of the membrane surface after the porous SSC layer was removed by ultrasonic agitation. d) EDX analysis of the sulfur content of various different areas. Scale bar: 2 μm.

perovskite-based MIEC membranes. This achievement is based on the identification of a new but potentially widespread low-temperature degradation mechanism in these materials which is driven by the segregation of sulfur impurities from the membrane bulk to the membrane surface, resulting in the accumulation of a blocking $BaSO_4$ surface phase. We have already demonstrated stable oxygen permeation fluxes of about $0.5\,mL\,cm^{-2}\,min^{-1}$ at 600 °C using 0.5 mm thick freestanding SSC-coated membranes. It is therefore reasonable to foresee that commercially significant ($>5\,mL\,cm^{-2}\,min^{-1}$) fluxes might be obtained at similar temperatures by applying the SSC-stabilization technique to asymmetric thin-film (about 20 μm in thickness) supported membranes, and the success in stabilization of the flux will open the door to many potential new applications for these membranes.

Received: November 13, 2012
Published online: February 10, 2013

Keywords: gas separation · membranes · metal oxides · oxygen permeation · perovskites

[1] a) J. P. Pérez-Ramírez, B. Vigeland, *Angew. Chem.* **2005**, *117*, 1136 – 1139; *Angew. Chem. Int. Ed.* **2005**, *44*, 1112 – 1115; b) A. Aguadero, H. Falcon, J. M. Campos-Martin, S. M. Al-Zahrani, J. L. G. Fierro, J. A. Alonso, *Angew. Chem.* **2011**, *123*, 6687 – 6691; *Angew. Chem. Int. Ed.* **2011**, *50*, 6557 – 6561.
[2] a) C. L. Jia, M. Lentzen, K. Urban, *Science* **2003**, *299*, 870 – 873; b) C. S. Chen, S. Ran, W. Liu, P. H. Yang, D. K. Peng, H. J. M. Bouwmeester, *Angew. Chem.* **2001**, *113*, 806 – 808; *Angew. Chem. Int. Ed.* **2001**, *40*, 784 – 786.
[3] Z. P. Shao, S. M. Haile, *Nature* **2004**, *431*, 170 – 173.
[4] a) Z. P. Shao, W. S. Yang, Y. Cong, H. Dong, J. H. Tong, G. X. Xiong, *J. Membr. Sci.* **2000**, *172*, 177 – 183; b) J. H. Tong, W. S. Yang, B. C. Zhu, R. Cai, *J. Membr. Sci.* **2002**, *203*, 175 – 189; c) J. Sunarsoa, S. Baumann, J. M. Serra, W. A. Meulenberg, S. Liu, Y. S. Lin, J. C. Diniz da Costa, *J. Membr. Sci.* **2008**, *320*, 13 – 41; d) H. Jiang, H. Wang, F. Liang, S. Werth, T. Schiestel, J. Caro, *Angew. Chem.* **2009**, *121*, 3027 – 3030; *Angew. Chem. Int. Ed.* **2009**, *48*, 2983 – 2986; e) H. Wang, S. Werth, T. Schiestel, J. Caro, *Angew. Chem.* **2005**, *117*, 7066 – 7069; *Angew. Chem. Int. Ed.* **2005**, *44*, 6906 – 6909; f) C. S. Chen, S. J. Feng, S. Ran, D. C. Zhu, W. Liu, H. J. M. Bouwmeester, *Angew. Chem.* **2003**, *115*, 5354 – 5356; *Angew. Chem. Int. Ed.* **2003**, *42*, 5196 – 5198; g) X. F. Zhu, Q. M. Li, Y. Cong, W. S. Yang, *Catal. Commun.* **2008**, *10*, 309 – 312; h) H. H. Wang, Y. Cong, W. S. Yang, *Chem. Commun.* **2002**, 1468 – 1469.
[5] a) S. Gopalan, H. Cui, *Int. J. Hydrogen Energy* **2004**, *29*, 1623 – 1629; b) H. Q. Jiang, H. H. Wang, S. Werth, T. Schiestel, J. Caro, *Angew. Chem.* **2008**, *120*, 9481 – 9484; *Angew. Chem. Int. Ed.* **2008**, *47*, 9341 – 9344.
[6] a) H. Luo, K. Efimov, H. Jiang, A. Feldhoff, H. Wang, J. Caro, *Angew. Chem.* **2011**, *123*, 785 – 789; *Angew. Chem. Int. Ed.* **2011**, *50*, 759 – 763; b) X. F. Zhu, H. Y. Liu, Y. Cong, W. S. Yang, *Chem. Commun.* **2012**, *48*, 251 – 253.
[7] O. Czuprat, S. Werth, J. Caro, T. Schiestel, *AIChE J.* **2010**, *56*, 2390 – 2396.
[8] a) E. Bucher, W. Sitte, *Solid State Ionics* **2011**, *192*, 480 – 482; b) E. Bucher, W. Sitte, F. Klauser, E. Bertel, *Solid State Ionics* **2011**, *191*, 61 – 67.
[9] a) S. Švarcová, K. Wiik, J. Tolchard, H. J. M. Bouwmeester, T. Grande, *Solid State Ionics* **2008**, *178*, 1787 – 1791; b) M. Arnold, T. M. Gesing, J. Martynczuk, A. Feldhoff, *Chem. Mater.* **2008**, *20*, 5851 – 5858.
[10] H. Kruidhof, H. J. M. Bouwmeester, R. H. E. Vondoorn, A. J. Burggraaf, *Solid State Ionics* **1993**, *63 – 65*, 816 – 822.
[11] a) J. O. Hong, O. Teller, M. Martin, H. I. Yoo, *Solid State Ionics* **1999**, *123*, 75 – 85; b) B. Wang, B. Zydorczak, D. Poulidi, I. S. Metcalfe, K. Li, *J. Membr. Sci.* **2011**, *369*, 526 – 535.
[12] H. Wang, C. Tablet, J. Caro, *J. Membr. Sci.* **2008**, *322*, 214 – 217.
[13] a) Q. M. Li, X. F. Zhu, Y. F. He, W. S. Yang, *Sep. Purif. Technol.* **2010**, *73*, 38 – 43; b) H. Cheng, X. Lu, D. Hu, Y. Zhang, W. Ding, H. Zhao, *Int. J. Hydrogen Energy* **2011**, *36*, 528 – 538.
[14] a) T. Ishihara, M. Honda, T. Shibayama, H. Minami, H. Nishiguchi, Y. Takita, *J. Electrochem. Soc.* **1998**, *145*, 3177 – 3183; b) H. Z. Zhang, W. S. Yang, *Chem. Commun.* **2007**, 4215 – 4217; c) X. F. Zhu, Q. M. Li, Y. Cong, W. S. Yang, *Solid State Ionics* **2011**, *185*, 27 – 31.

